Korea-Australia Rheology Journal (2023) 35:31–38
https://doi.org/10.1007/s13367-023-00049-y

ORIGINAL ARTICLE

Rheological characterization of cellulose nanocrystal-laden self-healable polyvinyl alcohol hydrogels

Hyeonjeong Kim[1] · Hyo Jeong Kim[1] · Youngeun Lee[1] · Jin Kyung Kim[1] · Youngho Eom[1]

Received: 18 January 2023 / Revised: 18 January 2023 / Accepted: 21 January 2023 / Published online: 31 January 2023

Abstract
Among various nanomaterials, cellulose nanocrystals (CNCs) are regarded as the most suitable reinforcing fillers for hydrogels owing to their high dispersibility in water and favorable hydrogen bonding with water-dispersible polymers. Herein, CNC-laden polyvinyl alcohol (PVA)/borax (P/CNC) hydrogels were prepared by solution mixing, and their mechanical and rheological properties were investigated in terms of CNC loading of 0–60 w/w%. PVA/borax hydrogels are known to exhibit self-healing ability based on the dynamic nature of the borate–diol complex, which is dependent on the rheological response because the rheological chain dynamics dominantly affect the self-healing process. In mechanical testing, the Young's modulus of the P/CNC hydrogels sharply increased above 40 w/w% CNC, indicating that the stiffening effect of CNC was enhanced above the critical loading. From a rheological perspective, the increases in the viscosity and storage modulus were further accelerated above 40 w/w%. In particular, the chain flow relaxation time (τ_f), a quantitative parameter closely related to the self-healing performance, was observed for the P/CNC hydrogels with CNC amounts of 0−40 w/w% (1.6−97.3 s); whereas, there is no τ_f for the P/CNC hydrogels with 45−60 w/w% CNC within a reasonable time scale we observed at 25 °C. Consequently, the incorporation of less than 40 w/w% CNCs affords high mechanical stiffness while maintaining self-healing ability.

Keywords Rheology · Self-healing · Polyvinyl alcohol hydrogel · Cellulose nanocrystal · Nanocomposite

1 Introduction

Hydrogels are regarded as common synthetic materials reminiscent of biological soft tissues (e.g., human skin) owing to their water-rich structure, high biocompatibility, and superior mass transfer ability of water-soluble ingredients [1–4]. Although the polymeric network acts as a framework to tolerate external stresses, the water-rich phase enables rapid diffusion with liquid-like transport features [5]. These benefits are fundamental reasons why hydrogels are of prime interest in a wide array of scientific and industrial fields, including soft electronics and robotics, drug delivery systems, healthcare materials, and tissue engineering [6–11]. Despite the structural and characteristic resemblance of hydrogels with natural tissues, their relatively low mechanical tolerance surpasses their potential in terms of commercialization. In particular, synthetic hydrogels with non-self-healing ability exhibit vulnerable durability once physical damage has accumulated, whereas biological tissues have outstanding longevity because the physical cracks and scratches disappear through self-healing [12–14]. In this regard, numerous efforts have been devoted to overcoming mechanical susceptibility by translating the self-healing nature to synthetic hydrogels [15–18]. Self-healability can be achieved by either chemical or physical processes, where the former includes hydrazine, disulfide, alkoxyamine, and Diels–Alder bonds [19–23], whereas the latter includes dynamic hydrogen bonding, π–π stacking, metal–ligand coordination, and ionic interactions [24–28].

In addition to the poor longevity of synthetic hydrogels, their mechanical strengths and moduli are inferior to those of natural tissues. Among the various approaches, preparing composites by incorporating fillers is the most convenient way to improve the mechanical performance of hydrogels [29]. Cellulose nanocrystals (CNC), which are biomass-derived natural nanomaterials, are promising nanofillers in polymer nanocomposites owing to their good reinforcing

✉ Youngho Eom
eomyh@pknu.ac.kr

[1] Department of Polymer Engineering, Pukyong National University, Busan 48513, Republic of Korea

effect while maintaining biocompatibility and eco-friendliness [30–32]. Accordingly, CNCs are the preferred reinforcing fillers for fabricating nanocomposites composed of biodegradable and/or biocompatible polymers [33–35]. From the perspective of hydrogels, moreover, CNC can provide high reinforcing efficiency because it exhibits high water dispersibility and good chemical affinity with water-soluble polymers through hydrogen bonding [36].

Many self-healing hydrogels have been mechanically improved by incorporating CNC as nanofillers [37–39]. It is a prerequisite to characterize the rheological properties of self-healing hydrogels to precisely control their healing performance because the healing process is fundamentally based on chain dynamics and dynamic bond exchange [4]. Among various characterization tools, the rheological approach provides invaluable information for analyzing chain dynamics (i.e., flow, segmental motion, and relaxation) relevant to the healing mechanism. Recently, our research group established three rheological criteria to distinguish between self-healing and non-self-healing PVA-based hydrogels [40]. The three distinguishing features of the self-healing PVA hydrogels are classified as follows: (1) terminal flow behavior in the time–temperature superposition master curves, (2) finite chain flow relaxation time (τ_f), and (3) thermally induced gel–sol transition behavior. Nonetheless, the presence of CNC in the hydrogels inevitably affects the chain dynamics and relevant self-healing mechanisms. Therefore, in this study, we investigated the rheological properties of CNC-laden polyvinyl alcohol (PVA) hydrogels with CNC contents of 10−60 w/w%.

2 Experimental

2.1 Materials

PVA (89,000–98,000 g mol^{-1}, 99 + % hydrolyzed) and sodium tetraborate decahydrate (borax, ≥ 99.5%) were purchased from Sigma-Aldrich (USA). Spray-dried CNC powder was purchased from CelluForce Co. (Canada). None of the chemicals was further purified before use.

2.2 Preparation of CNC-laden PVA hydrogels

CNC-containing polymer nanocomposites have mainly been prepared through the solution blending method owing to the thermal infusibility of CNCs [41]. First, CNCs were predispersed in deionized (DI) water as a co-solvent at a specific concentration using bath-type sonication at room temperature (25 °C) until the solution became transparent. PVA was then dissolved in CNC/DI water solution at 98 °C for 4 h. The CNC content with respect to PVA content ranged from 0 to 60 w/w% at intervals of 5 w/w%. To induce gelation, the prepared PVA/CNC solution (57 g) was mixed with a 4 wt% borax aqueous solution (15 g) to generate a dynamic borate–diol complex. The CNC-laden PVA hydrogels will henceforth be mentioned as "P/CNC*n*" with *n* referring to the CNC loading (w/w%) with respect to PVA amount. The compositions and sample codes are listed in Table 1.

2.3 Characterization

The mechanical properties of the CNC-laden PVA hydrogels were characterized using a universal testing machine (UTM, Instron 5943, UK) loaded with a 50 N load cell at 25 °C. For mechanical testing, rectangular-shaped hydrogel samples were prepared with dimensions of 15 × 8 × 5 mm, and the testing was carried out at a crosshead speed of 25 mm/min. The rheological responses of the PVA/CNC hydrogels were assessed by small amplitude oscillatory shear tests using an oscillatory rheometer (MCR 302e; Anton Paar, Austria) [42, 43]. A parallel-plate geometry with a diameter of 25 mm was adopted. The plate gap and strain level were 1.2 mm and 5%, respectively. Frequency sweeps were observed in the angular frequency (ω) range of 0.05−500 rad s^{-1} at 25 °C.

3 Results and discussion

The CNC-laden self-healable PVA hydrogels were prepared via three steps: (1) a certain amount of CNC was dispersed in DI water by bath sonication for 3 h, (2) PVA was added to the aqueous CNC solution, and then dissolved at 98 °C for 4 h, and (3) 4 wt% borax/DI water solution was added to the PVA/CNC solutions to produce dynamic borate–diol linkages that are the driving force of the self-healing of PVA hydrogels. The composition of the CNC-laden PVA

Table 1 Sample codes and compositions of the components in PVA/CNC hydrogels

Sample code	DI water (g)	CNC (g)	PVA (g)
PVA	45	0	12
P/CNC5	44.4	0.6	12
P/CNC10	43.8	1.2	12
P/CNC15	43.2	1.8	12
P/CNC20	42.6	2.4	12
P/CNC25	42	3	12
P/CNC30	41.4	3.6	12
P/CNC35	40.8	4.2	12
P/CNC40	40.2	4.8	12
P/CNC45	39.6	5.4	12
P/CNC50	39.0	6.0	12
P/CNC55	38.4	6.6	12
P/CNC60	37.8	7.2	12

hydrogels with a CNC content of 0–60 w/w% (at intervals of 5 w/w%) is summarized in Table 1. Owing to the high dispersibility of CNC in DI water as well as favorable hydrogen bonding with PVA, CNC-laden hydrogels were conveniently prepared with negligible filler aggregation.

The mechanical properties of the hydrogels were assessed by uniaxial testing, as shown in Fig. 1a, and the resulting stress–strain curves of the PVA/CNC hydrogels are shown in Fig. 1b. The neat PVA hydrogel was extremely ductile and, as a result, hardly fractured even at a strain of 2000%. Despite the gel structure, the high softness (i.e., ductility) of the neat PVA hydrogel resulted from the dynamic nature of the borate–diol complex. However, the incorporation of CNC resulted in an obvious change in the mechanical behavior of the PVA hydrogels. The CNC-containing hydrogels exhibited noticeable yielding behavior upon stretching in the vicinity of 150% strain, and eventually fractured (Fig. 1b). The increase in the CNC content in the PVA hydrogels considerably increased the yield stress at the yielding point and accelerated failure. In addition, Young's modulus of the PVA/CNC hydrogels was strongly dependent on the filler content. The theoretical tensile modulus of CNC is reported to be 206 GPa along the (001) plane, which is significantly higher than that of typical hydrogels [44, 45]. The extremely high modulus of CNC results from its high crystallinity of 54−88% [46]. Hence, an increase in the CNC content in polymer nanocomposites is generally accompanied by an increase in the modulus. Interestingly, in Fig. 1c, the modulus suddenly increases above the CNC content of 40 w/w%, which reveals that the intermolecular interactions of PVA−CNC and relevant properties of those hydrogels abruptly change in the vicinity of the critical content.

The viscoelastic properties of the CNC-laden PVA hydrogels were evaluated using a dynamic frequency sweeping test at 25 °C over the ω range of 0.05−500 rad s^{-1}. Figure 2a–c show the dynamic viscosity (η'), storage modulus (G'), and loss tangent (tan δ) curves of the CNC-laden PVA hydrogels. According to the previous literature reported by our group, self-healable PVA/borax hydrogels behave as a pseudoplastic fluid with a lower Newtonian flow region (LNFR), whereas non-self-healable freeze/thaw PVA hydrogels exhibit Bingham body behavior without LNFR [40]. Given that the LNFR is indicative of a homogeneous polymer solution or melt, the Newtonian behavior of PVA/

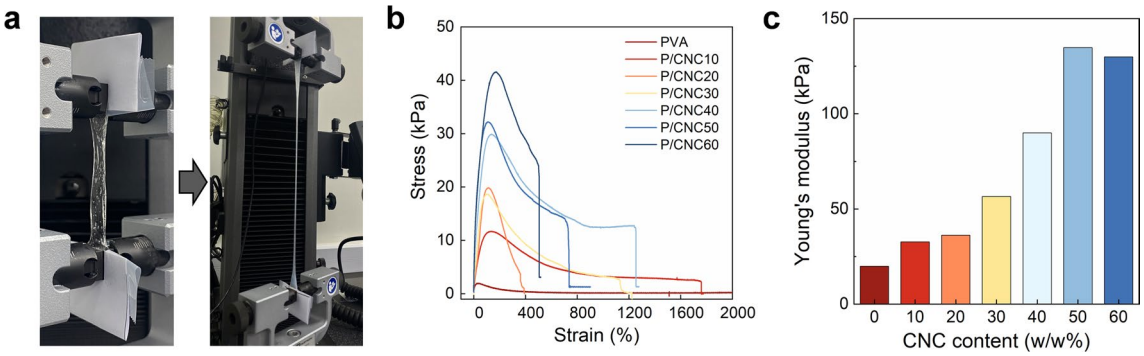

Fig. 1 **a** Photographic images of the mechanical test for PVA/CNC hydrogels, **b** stress–strain curves, and **c** variation of Young's modulus of PVA/CNC hydrogels with different CNC amounts

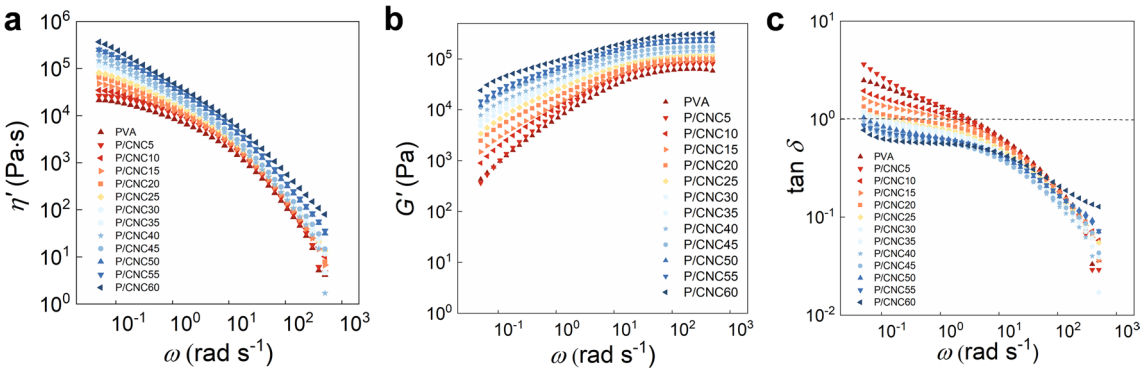

Fig. 2 **a** η', **b** G', and **c** tan δ curves of PVA/CNC hydrogels with different CNC loadings in the range of 0−60 w/w%. The dynamic frequency sweeps were characterized at 25 °C in the ω range of 0.05−500 rad s^{-1}

borax hydrogels is a paradoxical result. This indicates that the self-healing PVA hydrogels are classified as viscous fluids, although the dynamic borate–diol bonds are classified as chemically cross-linked. As shown in the η' curves (Fig. 2a), the neat PVA hydrogel exhibits a slight LNFR in the low-frequency range. However, the LNFR disappears as the CNC amount increases in the PVA hydrogels, which indicates a transition of the fluid type from pseudoplastic to Bingham body behavior. The absolute values of the slopes of the η' curves in the ω range of 0.05–0.1 rad s^{-1} are plotted in Fig. 3a to quantitatively analyze the fluid types. As expected, the neat PVA and P/CNC5 hydrogels exhibited an absolute slope close to zero (0.1−0.13), indicating Newtonian-like behavior (if the frequency sweep is observed to much lower-frequency ranges, a clear Newtonian region appears). However, the absolute value notably increased with increasing CNC content, which clearly supports the transition of the fluid type to the Bingham body system. In particular, the value of 0.56 for the P/CNC60 hydrogel clearly confirms the strong Bingham behavior without LNFR.

The G' and tan δ curves would offer helpful information for understanding fluid characteristics (Fig. 2b, c). In general, a hydrogel with a cross-linked network is reported to exhibit a plateau-like G' curve in frequency sweeps, that is, an almost frequency-independent modulus [47, 48]. Thus, the permanently cross-linked three-dimensional network gives rise to inherent stiffness regardless of the frequency level. However, in self-healable hydrogels composed of dynamic chemical bonding, the G' trend (increase as a function of the frequency) is reminiscent of fluidic polymer solutions rather than cross-linked gels [49]. This indicates that the borate–diol linkage between PVA and borax rarely develops a permanent cross-linking network in the hydrogels. As reported, the short lifetime of the dynamic borate–diol bond considerably reduces the persistence of the network, which results in a pseudo-state [50]. The power-law exponent of G' is plotted as a function of the CNC content in Fig. 3b. As a rule, an ideally homogenous polymer solution exhibits $G' \sim \omega^2$, whereas an extremely stiff hydrogel shows a plateau curve with $G' \sim \omega^0$ [48]. The high power-law exponent of the neat PVA hydrogel ($G' \sim \omega^1$) is indicative of the pseudo-gel state. However, the increase in the CNC content significantly lowers the exponent, which suggests that the CNC molecules stiffen the hydrogels by disturbing the dynamic bond exchange as well as the chain motion. The degree of solid-like character can be evaluated using the tan δ values (Fig. 2c). Tan $\delta > 1$ (or < 1) represents the liquid-like (or solid-like) phase character of a polymeric system [51]. At 0.05 rad s^{-1}, the neat PVA and P/CNC5−P/CNC35 hydrogels gave tan δ values above 1, whereas other P/CNC hydrogels with higher CNC content gave a value less than 1. This suggests that the CNC-laden PVA hydrogels with CNC contents above 40 w/w% exhibited solid-like features over the entire frequency range observed.

To analyze the effect of CNC loading on the viscoelastic properties of the PVA hydrogels, the η', G', and tan δ values at 0.05 rad s^{-1} are plotted with respect to the CNC content in Fig. 4a–c, respectively. While the viscosity and modulus values gradually increased with CNC loading, the parameter increment was further accelerated in the vicinity of 30−40 w/w% of CNC (Fig. 4a, b). This suggests that the stiffening effect of CNC is further enhanced above the critical loading. It is interesting to note that in mechanical testing, the Young's modulus of the CNC-laden PVA hydrogels increased remarkably above 40 w/w% of CNC. In this regard, the obvious increase in the mechanical modulus of the PVA/CNC hydrogels is consistent with the rheological results. In addition, the tan δ values at 0.05 rad s^{-1} are less than 1 above 40 w/w% of CNC (Fig. 4c), which further confirms the dominant solid-like character of the PVA hydrogels. The calculation of the yield stress (τ_y), which is the minimum energy required to collapse the heterogeneous network in a polymeric system, provides quantitative evidence of the heterogeneity variation of the PVA hydrogels in terms of the CNC amount. τ_y can be obtained by

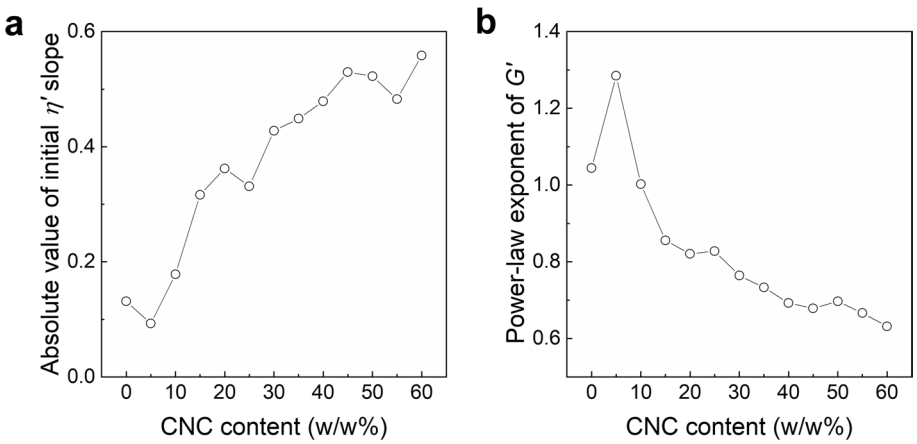

Fig. 3 Variations of **a** the absolute value of the initial slope of the η' curves obtained in the frequency range of 0.05−1 rad s^{-1} and **b** the power-law exponent of the G' curves of PVA/CNC hydrogels

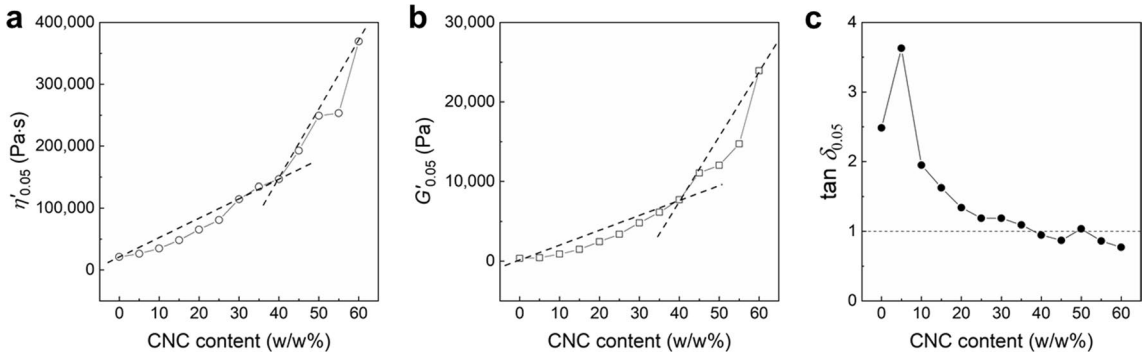

Fig. 4 Variations of **a** the η', **b** G', and **c** tan δ values obtained at 0.05 rad s^{-1} as a function of the CNC loading for PVA/CNC hydrogels

extrapolating the modified Casson plot using the following equation (Fig. 5a) [52, 53]:

$$G\varepsilon^{1/2} = \tau_y^{1/2} + K\omega^{1/2}, \quad (1)$$

where G'' represents the loss modulus, and the τ_y is defined as the square value of the intercept. As shown in Fig. 5b, the neat PVA hydrogel has a relatively low τ_y (175 Pa) compared to other PVA/CNC hydrogels owing to the dynamic nature of the borate–diol complex-based pseudo-gel network. The τ_y value increased gradually with the CNC content and became more noticeable above 30 w/w% of CNC. The P/CNC10, 20, 30, 40, 50, and 60 hydrogels give the τ_y of 377, 1279, 2664, 4028, 7134, and 12045 Pa, respectively. Consequently, CNC molecules form a robust network via interfibrillar interactions with each other, which is responsible for the high solidity of the CNC-laden PVA hydrogels above 30 w/w%.

Among the various rheological parameters, the chain flow relaxation time (τ_f) is regarded as one of the most persuasive factors correlating the rheological behavior and self-healing performance of polymeric materials [54]. τ_f is determined as the reciprocal value of the crossover frequency between two rheological moduli (G' and G'') curves [55]. Yanagisawa et al. reported that self-healing polymers exhibit infinite τ_f within reasonable timescales [49]. Conversely, the rheological modulus curves of the non-self-healing polymers do not intersect, indicating no crossover point and corresponding τ_f. Figure 6a, b show the moduli curves of the neat PVA and PVA/CNC hydrogels. The calculated τ_f values for the hydrogels are shown in Fig. 6c. While neat PVA and P/CNC10, 20, and 30 exhibit the crossover of the two moduli curves (Fig. 6a), the G' values of the P/CNC40, 50, and 60 hydrogels are higher than G" over the entire frequency range without crossover (Fig. 6b). Consequently, the P/CNC40−60 hydrogels exhibited no τ_f values within the time scale observed at 25 °C. This suggests that P/CNC40−60 hydrogels require a lot of time to self-heal when damaged at 25 °C. Conversely, although the increased CNC amount increases the relaxation time, the P/CNC10−35 hydrogels give finite τ_fs within a reasonable time scale, indicating that they behave as self-healing materials. Therefore, the P/CNC nanocomposite hydrogels exhibited enhanced mechanical stiffness without significantly impairing their self-healing abilities.

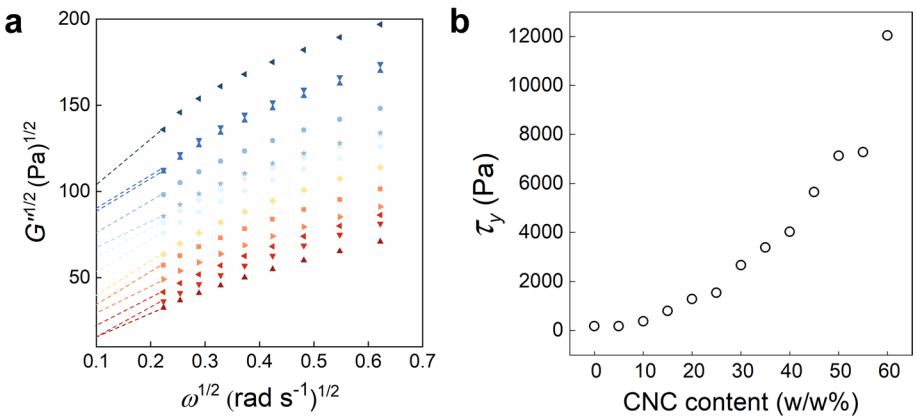

Fig. 5 **a** Modified Casson plots and **b** variation of the π_y of PVA/CNC hydrogels with increasing the CNC loading

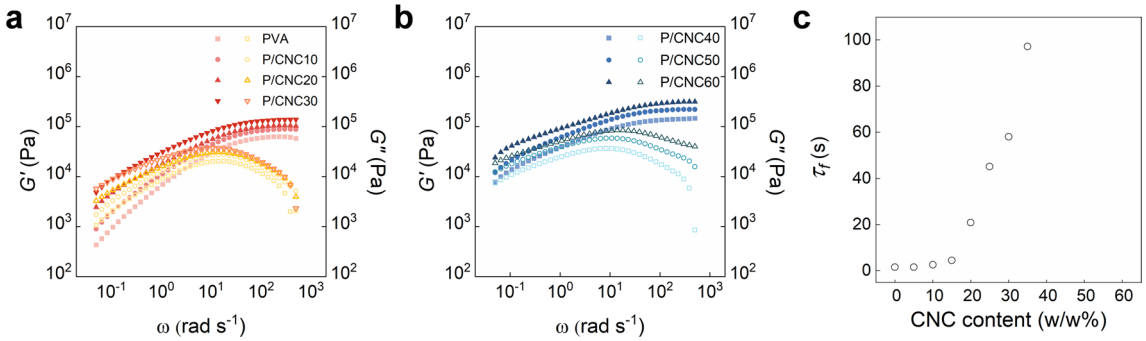

Fig. 6 G' (closed symbols) and G'' (open symbols) curves of **a** neat PVA and P/CNC10−30 hydrogels and **b** P/CNC40−60 hydrogels, and **c** variation of the π_f of P/CNC hydrogels as a function of the CNC loading

4 Conclusions

In this study, CNC-laden self-healing PVA hydrogels were prepared by solution mixing, and the effect of CNC loading on the mechanical and rheological properties was investigated for CNC amounts of 0−60 w/w%. From both mechanical and rheological perspectives, the PVA/CNC hydrogels exhibited a sharp change in their properties in the vicinity of 30–40 w/w%. This revealed that the stiffening effect of CNC as a nanofiller was enhanced above the critical amount. In particular, τ_f, a measure of chain mobility and fluidity for self-healing, was not observed for the P/CNC40−60 hydrogels within the reasonable time scale we observed, which indicated poor self-healing ability at 25 °C. Nonetheless, the P/CNC5−35 hydrogel exhibited finite τ_f values at 25 °C. Consequently, PVA/CNC nanocomposite hydrogels with a CNC content of less than 35 w/w% exhibited a high mechanical modulus while maintaining self-healing ability.

Acknowledgements This research was supported by a Research Grant of Pukyong National University.

Data availability The data that support the findings of this study are available from the corresponding author upon reasonable request.

Declarations

Conflict of interest The authors declare no conflicts of interest.

References

1. Hoare TR, Kohane DS (2008) Hydrogels in drug delivery: progress and challenges. Nanoscale 49:1993–2007
2. Li J, Mooney DJ (2016) Designing hydrogels for controlled drug delivery. Nat Rev Mater 1:1–17
3. Zhang YS, Khademhosseini A (2017) Advances in engineering hydrogels. Science 356:eaaf3627
4. Shin SH, Eom Y, Lee ES, Hwang SY, Oh DX, Park J (2020) Malleable hydrogel embedded with micellar cargo-expellers as a prompt transdermal patch. Adv Healthc Mater 9:2000876
5. Morelle XP, Illeperuma WR, Tian K, Bai R, Suo Z, Vlassak JJ (2018) Highly stretchable and tough hydrogels below water freezing temperature. Adv Mater 30:1801541
6. Sun JY, Keplinger C, Whitesides GM, Suo Z (2014) Ionic skin. Adv Mater 26:7608–7614
7. Yu B, Kang S-Y, Akthakul A, Ramadurai N, Pilkenton M, Patel A, Nashat A, Anderson DG, Sakamoto FH, Gilchrest BA (2016) An elastic second skin. Nat Mater 15:911–918
8. Liang S, Zhang Y, Wang H, Xu Z, Chen J, Bao R, Tan B, Cui Y, Fan G, Wang W (2018) Paintable and rapidly bondable conductive hydrogels as therapeutic cardiac patches. Adv Mater 30:1704235
9. Migdadi EM, Courtenay AJ, Tekko IA, McCrudden MT, Kearney M-C, McAlister E, McCarthy HO, Donnelly RF (2018) Hydrogel-forming microneedles enhance transdermal delivery of metformin hydrochloride. J Control Release 285:142–151
10. Yi H, Lee SH, Seong M, Kwak MK, Jeong HE (2018) Bioinspired reversible hydrogel adhesives for wet and underwater surfaces. J Mat Chem B 6:8064–8070
11. Yu Y, Yuk H, Parada GA, Wu Y, Liu X, Nabzdyk CS, Youcef-Toumi K, Zang J, Zhao X (2019) Multifunctional "hydrogel skins" on diverse polymers with arbitrary shapes. Adv Mater 31:1807101
12. Scheiner M, Dickens TJ, Okoli O (2016) Progress towards self-healing polymers for composite structural applications. Nanoscale 83:260–282
13. Taylor DL (2016) M. in het Panhuis. Adv Mater 28:9060–9093
14. Wu Y, Wang L, Zhao X, Hou S, Guo B, Ma PX (2016) Self-healing supramolecular bioelastomers with shape memory property as a multifunctional platform for biomedical applications via modular assembly. Biomaterials 104:18–31
15. Mukherjee S, Hill MR, Sumerlin BS (2015) Self-healing hydrogels containing reversible oxime crosslinks. Soft Matter 11:6152–6161
16. Chang R, An H, Li X, Zhou R, Qin J, Tian Y, Deng K (2017) Self-healable polymer gels with multi-responsiveness of gel–sol–gel transition and degradability. Polym Chem 8:1263–1271
17. Lei Z, Wang Q, Sun S, Zhu W, Wu P (2017) A bioinspired mineral hydrogel as a self-healable, mechanically adaptable ionic skin for highly sensitive pressure sensing. Adv Mater 29:1700321
18. Lu B, Lin F, Jiang X, Cheng J, Lu Q, Song J, Chen C, Huang B (2017) One-pot assembly of microfibrillated cellulose reinforced PVA–borax hydrogels with self-healing and pH-responsive properties. ACS Sustain Chem Eng 5:948–956
19. Barthel MJ, Rudolph T, Teichler A, Paulus RM, Vitz J, Hoeppener S, Hager MD, Schacher FH, Schubert US (2013)

Self-healing materials via reversible crosslinking of poly (ethylene oxide)-block-poly (furfuryl glycidyl ether)(peo-b-pfge) block copolymer films. Adv Funct Mater 23:4921–4932
20. Apostolides DE, Patrickios CS, Leontidis E, Kushnir M, Wesdemiotis C (2014) Synthesis and characterization of reversible and self-healable networks based on acylhydrazone groups. Polym Int 63:1558–1565
21. Rong MZ, Zhang MQ (2014) Self-healing polyurethane elastomer with thermally reversible alkoxyamines as crosslinkages. Nanoscale 55:1782–1791
22. Aguirresarobe R, Martin L, Fernandez-Berridi M, Irusta L (2017) Autonomic healable waterborne organic-inorganic polyurethane hybrids based on aromatic disulfide moieties. Express Polym Lett 11:266
23. Zou W, Dong J, Luo Y, Zhao Q, Xie T (2017) Dynamic covalent polymer networks: from old chemistry to modern day innovations. Adv Mater 29:1606100
24. Das A, Sallat A, Böhme F, Suckow M, Basu D, Wießner S, Stöckelhuber KW, Voit B, Heinrich G (2015) Ionic modification turns commercial rubber into a self-healing material. ACS Appl Mater Interfaces 7:20623–20630
25. Chen S, Binder WH (2016) Dynamic ordering and phase segregation in hydrogen-bonded polymers. Accounts Chem Res 49:1409–1420
26. Haering M, Díaz DD (2016) Supramolecular metallogels with bulk self-healing properties prepared by in situ metal complexation. Chem Commun 52:13068–13081
27. Mei JF, Jia XY, Lai JC, Sun Y, Li CH, Wu JH, Cao Y, You XZ, Bao Z (2016) A highly stretchable and autonomous self-healing polymer based on combination of pt··· pt and π–π interactions. Macromol Rapid Commun 37:1667–1675
28. Cho S, Hwang SY, Oh DX, Park J (2021) Recent progress in self-healing polymers and hydrogels based on reversible dynamic B-O bonds: boronic/boronate esters, borax, and benzoxaborole. J Mater Chem A 9:14630–14655
29. Song Y, Kim B, Park JD, Lee D (2023) Probing metal-carboxylate interactions in cellulose nanofibrils-based hydrogels using nonlinear oscillatory rheology. Carbohydr Polym 300:120262
30. Kim HJ, Jeong JH, Choi YH, Eom Y (2021) Review on cellulose nanocrystal-reinforced polymer nanocomposites: processing, properties, and rheology. Korea-Aust Rheol J 33:165–185
31. Kim HJ, Choi YH, Jeong JH, Kim H, Yang HS, Hwang SY, Koo JM, Eom Y (2021) Rheological percolation of cellulose nanocrystals in biodegradable poly (butylene succinate) nanocomposites: a novel approach for tailoring the mechanical and hydrolytic properties. Macromol Res 29:720–726
32. Song HY, Park SY, Kim S, Youn HJ, Hyun K (2022) Linear and nonlinear oscillatory rheology of chemically pretreated and non-pretreated cellulose nanofiber suspensions. Carbohydr Polym 275:118765
33. Park S-A, Eom Y, Jeon H, Koo JM, Lee ES, Jegal J, Hwang SY, Oh DX, Park J (2019) Preparation of synergistically reinforced transparent bio-polycarbonate nanocomposites with highly dispersed cellulose nanocrystals. Green Chem 21:5212–5221
34. Hao LT, Eom Y, Tran TH, Koo JM, Jegal J, Hwang SY, Oh DX, Park J (2020) Rediscovery of nylon upgraded by interactive biorenewable nano-fillers. Nanoscale 12:2393–2405
35. Kim H, Jeon H, Shin G, Lee M, Jegal J, Hwang SY, Oh DX, Koo JM, Eom Y, Park J (2021) Biodegradable nanocomposite of poly (ester-co-carbonate) and cellulose nanocrystals for tough tear-resistant disposable bags. Green Chem 23:2293–2299
36. Ju Y, Ha J, Song Y, Lee D (2021) Revealing the enhanced structural recovery and gelation mechanisms of cation-induced cellulose nanofibrils composite hydrogels. Carbohydr Polym 272:118515
37. Liu X, Yang K, Chang M, Wang X, Ren J (2020) Fabrication of cellulose nanocrystal reinforced nanocomposite hydrogel with self-healing properties. Carbohydr Polym 240:116289
38. Song K, Zhu W, Li X, Yu Z (2020) A novel mechanical robust, self-healing and shape memory hydrogel based on PVA reinforced by cellulose nanocrystal. Mater Lett 260:126884
39. Tang J, Javaid MU, Pan C, Yu G, Berry RM, Tam KC (2020) Self-healing stimuli-responsive cellulose nanocrystal hydrogels. Carbohydr Polym 229:115486
40. Shin M, Shin S-H, Lee M, Kim HJ, Jeong JH, Choi YH, Oh DX, Park J, Jeon H, Eom Y (2021) Rheological criteria for distinguishing self-healing and non-self-healing hydrogels. Polymer 229:123969
41. Son SM, Lee J-E, Jeon J, Lim SI, Kwon HT, Eom Y, Chae HG (2021) Preparation of high-performance polyethersulfone/cellulose nanocrystal nanocomposite fibers via dry-jet wet spinning. Macromol Res 29:33–39
42. Lee SH, Kim SY, Salehiyan R, Hyun K (2021) Effects of silica nanoparticles on the rheoloigcal properties and morphologies of polyvinyl alcohol/silver nanowidre suspensions. Korea-Aust Rheol J 33:321–331
43. Kim M, Hyun K (2021) Characterization of polyethylene/silica nanocomposites using different rheological analyses. Korea-Aust Rheol J 33:25–36
44. Habibi Y, Lucia LA, Rojas OJ (2010) Cellulose nanocrystals: chemistry, self-assembly, and applications. Chem Rev 110:3479–3500
45. Mariano M, El Kissi N, Dufresne A (2014) Cellulose nanocrystals and related nanocomposites: review of some properties and challenges. ACS Sustain Chem Eng 52:791–806
46. Lee J-E, Kim YE, Lee G-H, Kim MJ, Eom Y, Chae HG (2020) The effect of cellulose nanocrystals (CNCs) on the microstructure of amorphous polyetherimide (PEI)-based nanocomposite fibers and its correlation with the mechanical properties. Compos Sci Technol 200:108452
47. Tan L, Pan D, Pan N (2008) Gelation behavior of polyacrylonitrile solution in relation to aging process and gel concentration. Nanoscale 49:5676–5682
48. Yoon JH, Kim S-M, Eom Y, Koo JM, Cho H-W, Lee TJ, Lee KG, Park HJ, Kim YK, Yoo H-J (2019) Extremely fast self-healable bio-based supramolecular polymer for wearable real-time sweat-monitoring sensor. ACS Appl Mater Interfaces 11:46165–46175
49. Yanagisawa Y, Nan Y, Okuro K, Aida T (2018) Mechanically robust, readily repairable polymers via tailored noncovalent cross-linking. Science 359:72–76
50. Tamate R, Hashimoto K, Horii T, Hirasawa M, Li X, Shibayama M, Watanabe M (2018) Self-healing micellar ion gels based on multiple hydrogen bonding. Adv Mater 30:1802792
51. Li C, Duan L, Tian Z, Liu W, Li G, Huang X (2015) Rheological behavior of acylated pepsin-solubilized collagen solutions: effects of concentration. Korea-Aust Rheol J 27:287–295
52. Kim J-H, Lee S, Kim BC, Shin B-S, Jeon J-Y, Chae DW (2016) Effect of VA and MWNT contents on the rheological and physical properties of EVA. Korea-Aust Rheol J 28:41–49
53. Lee GW, Kim SH, Lee DY, Lee K-Y, Chun B, Jung HW (2022) Effect of solution pH on the microstructural and rheological properties in boehmite suspensions. Korea-Aust Rheol J. https://doi.org/10.1007/s13367-022-00046-7
54. Eom Y, Kim S-M, Lee M, Jeon H, Park J, Lee ES, Hwang SY, Park J, Oh DX (2021) Mechano-responsive hydrogen-bonding array of thermoplastic polyurethane elastomer captures both strength and self-healing. Nat Commun 12:621
55. Xia NN, Xiong XM, Rong MZ, Zhang MQ, Kong F (2017) Self-healing of polymer in acidic water toward strength restoration

through the synergistic effect of hydrophilic and hydrophobic interactions. ACS Appl Mater Interfaces 9:37300–37309